AIAA-91-2502

Enhanced Capability of the Combustion-Heated Scramjet Test Facility

Kenneth E. Rock, Earl H. Andrews, and
James M. Eggers
NASA Langley Research Center
Hampton, VA

AIAA/SAE/ASME/ASEE
27th Joint Propulsion Conference

June, 24-26, 1991/Sacramento, CA

For permission to copy or republish, contact the American Institute of Aeronautics and Astronautics
370 L'Enfant Promenade, S.W., Washington, D.C. 20024

ENHANCED CAPABILITY OF THE COMBUSTION-HEATED SCRAMJET TEST FACILITY

Kenneth E. Rock*
Earl H. Andrews**
and
James M. Eggers***
NASA Langley Research Center
Hampton, Virginia

AIAA/ASME/SAE 27th Joint Propulsion Conference and Exhibit
Sacramento, California
June 24-27, 1991

ABSTRACT

The Hypersonic Propulsion Branch at the NASA Langley Research Center has focused its research toward the supersonic-combustion ramjet (scramjet) airframe-integrated propulsion system concept since the late 1960's. For over 14 years, subscale, hydrogen-burning, component-integration engine models have been tested in two different Langley scramjet test facilities at simulated Mach 4 to 8 flight conditions. The past 2 years have been devoted entirely to tests of National Aero-Space Plane engine concepts. One of the test facilities, the Combustion-Heated Scramjet Test Facility (CHSTF), has recently been upgraded to expand its operational envelope.

The CHSTF was originally limited to a total pressure of 190 psia and a total temperature of 2250° R because of heater duct safety considerations. The addition of a new facility heater increased the total pressure capability to 500 psia and the total temperature capability to 3000° R, but altitude and Mach number simulation were still limited by the air ejector-aided atmospheric exhaust system. A new 70-foot vacuum-sphere/steam ejector system and a new Mach 4.7 nozzle (in addition to an existing Mach 3.5 nozzle) have greatly expanded the facility altitude/Mach number simulation envelope. The reduced exhaust pressure capability has increased the altitude simulation range from 30-80 Kft to 30-120 Kft; the reduced exhaust pressure along with the new heater and Mach 4.7 nozzle has increased flight Mach number simulation from Mach 4 to Mach 6.

The CHSTF, along with the Arc-Heated Scramjet Test Facility (AHSTF) and the 8-Foot High-Temperature Tunnel (8'HTT), are the facilities of the NASA Langley scramjet test complex. With the CHSTF modifications complete and the modifications to NASA Langley's 8-Foot High-Temperature Tunnel to make it suitable to scramjet propulsion tests near completion, the simulation envelopes of these facilities now overlap. This overlap is a valuable asset in that tests at similar simulated flight conditions in different facilities can provide a basis for comparison which will help the understanding of how tunnel flow contaminants and scale affect engine performance.

This paper will describe the CHSTF and its modifications, and will document the expanded simulation capabilities of the facility. Nozzle exit surveys and tunnel calibration information will be presented and discussed.

NOMENCLATURE

H	enthalpy, Btu/lbs
M	Mach number
P	pressure, psia
T	temperature, °R
$\dot{w}$	flow rate, lbm/s
ϕ	fuel equivalence ratio
ρ	density, lbm/ft^3

Subscripts

t	total or stagnation condition
1	condition behind vehicle bow shock or at facility nozzle exit
brn	burner or heater
ej	ejector
noz	nozzle exit

* Aerospace Research Engineer, Hypersonic Propulsion Branch, Member AIAA.
** Senior Research Scientist, Hypersonic Propulsion Branch, Senior Member AIAA.
*** Senior Research Scientist, Hypersonic Propulsion Branch

Copyright ©1991 by the American Institute of Aeronautics and Astronautics, Inc. No copyright is asserted in the United States under Title 17, U.S. Code. The U.S. Government has a royalty-free license to exercise all rights under the copyright claimed herein for Governmental purposes. All other rights are reserved by the copyright owner.

INTRODUCTION

Interest in airbreathing hypersonic propulsion in the United States began in the late 1950's, and NASA Langley's involvement in this area dates back to the early 1960's when research was focused on the Hypersonic Research Engine (HRE).[1-3] This early work demonstrated the feasibility of the ramjet/scramjet engine cycle, and continued analyses showed that a viable scramjet engine design would have to be blended with the airframe to avoid high installation drag. In 1968, the Hypersonic Propulsion Branch (HPB) at the NASA Langley Research Center initiated a program to study ramjet/scramjet propulsion systems that were highly integrated with the vehicle to produce high installed thrust by using the aircraft forebody as an inlet precompression surface and the aircraft aft end as a nozzle expansion surface, thereby effectively utilizing the entire undersurface of the vehicle to process the flow[4] (Figure 1). The propulsion system concept features a cluster of individual rectangular engine modules of size and shape suitable for ground testing.

In the mid-1970's, two existing facilities at NASA Langley were modified to allow tests of subscale, component-integration models of airframe-integrated scramjets at simulated flight conditions ranging from Mach 3.5 to Mach 8. These two facilities, the Combustion-Heated Scramjet Test Facility[5] (CHSTF) and the Arc-Heated Scramjet Test Facility[6,7] (AHSTF), were utilized in the testing of four different engine concepts involving more than 1000 tests during the period from December 1976 to May 1988. Results from three of these engine tests are summarized in reference 8. In May of 1988, with the emergence of the National Aero-Space Plane (NASP) Program, these facilities were dedicated to the testing of NASP engine concepts. During the period from May 1988 to September 1990, an additional 1000 tests were performed in the two Langley facilities using five engine concepts evolved by the prime NASP contractors, Rocketdyne and Pratt and Whitney, a NASP Government Baseline Engine Model, and one Johns Hopkins University/Applied Physics Laboratory (JHU/APL) model.

In early 1991, modifications to the CHSTF were completed which greatly enhance the test capabilities of that facility; systems shakedown is currently underway. A new facility heater has been installed which extends the previous stagnation pressure limit of 190 psia and stagnation temperature limit of 2250° R to 500 psia and 3000° R,[9] respectively. When these limits are coupled with a new Mach 4.7 nozzle, flight Mach number simulation is increased from the nominal Mach 4 condition (present Mach 3.5 nozzle) to Mach 6. A vacuum sphere/steam ejector exhaust system has also been installed which increases altitude simulation capability from 80,000 feet to 120,000 feet, reduces facility/model interaction, and significantly reduces facility air usage by eliminating dependence on an air ejector as a vacuum sink. The CHSTF physical modifications, its increased simulation capabilities, and calibration data obtained to date will be presented and discussed in this paper.

PROPULSION TEST FACILITIES

While aerodynamic test facilities strive to produce proper Reynolds numbers and Mach numbers, propulsion test facilities involving combustion must duplicate flight total enthalpy, and the test gas must have the proper oxygen content. Flight total enthalpy duplication and a facility stagnation pressure which is consistent with the simulated flight altitude are necessary since the combustion kinetics of the fuel/air mixture depend strongly on the static pressure, static temperature, and velocity of the test gas. Test gas total enthalpies required for scramjet propulsion testing in simulation of supersonic to orbital speeds are currently generated in combustion-, arc-, and convection-heated flows, and in shock tunnels and expansion tubes. The Combustion-Heated Scramjet Facility heats the test gas by burning hydrogen in oxygen-enriched air and the Arc-Heated Scramjet Test Facility heats the test gas by passing air through an electric arc. In addition, NASA Langley's 8'HTT is currently undergoing modifications to add oxygen replenishment to its methane/air heater to make the facility suitable for scramjet combustion testing.[10,11] The simulation capabilities in terms of altitude, Mach number, and dynamic pressure simulation for the CHSTF, AHSTF, and 8'HTT are shown in Figure 2.[12]

Subscale Scramjet Engine Testing

The Hypersonic Propulsion Branch has assembled a group of propulsion facilities that enables the testing of separate engine components as well as complete subscale engine models.[13] These facilities, together with other Langley aerodynamic facilities, comprise the Langley Scramjet Test Complex.[12]

Small-scale inlet experiments are performed in the HPB Mach 4 Blowdown Facility which uses unheated air as the test gas and has a 9- by 9-inch nozzle exit. Other aerodynamic test facilities at Langley are utilized for inlet tests across the speed range. These include the Unitary Plan Wind Tunnel (Mach = 1.5 to 4.6), the 20-Inch Mach 6 Tunnel, the 31-Inch Mach 10 Tunnel, the Mach 17 Nitrogen Tunnel and the Mach 17 and 22 Helium Tunnels. These tests yield information about inlet starting characteristics, mass capture, surface pressure distributions, tolerable combustor pressure levels, etc. Small-scale, direct-connect combustor tests that simulate all or a portion of the engine combustor are conducted in Langley's Direct-Connect Supersonic Combustion Test Facility (DCSCTF) to provide basic research information on supersonic fuel-air mixing, ignition, and combustion processes.[14] Enthalpy levels in this facility simulate flight speeds up to Mach 8.

While individual engine component tests yield valuable basic research information, a new set of problems may be

encountered when these components are integrated into an engine configuration. Inlet component tests may include artificial back pressuring to simulate the pressure rise due to combustion, but the mechanisms for feeding this pressure forward and its effect on the inlet may be different in an engine configuration where the back pressure is due to combustion. Flow conditions supplied to direct-connect combustor tests are generally shock-free and uniform, while the flow delivered by an inlet attached to a combustor in an engine configuration includes reflected shocks and flow nonuniformity. It is therefore necessary to test these components in an integrated fashion, representing a true engine flowpath, to resolve interactions between the various engine components and to determine the overall engine performance. It is this function that the CHSTF and AHSTF, and, on a larger scale, the 8'HTT serve with tests simulating flight speeds up to Mach 8 and Mach 7, respectively.

Flight Simulation Logic

In subscale scramjet engine tests, flight conditions of an airframe-integrated scramjet must be simulated as closely as possible. The simulation logic used in both the CHSTF and the AHSTF is depicted in Figure 3. A vehicle flying at supersonic speeds compresses the flow across the forebody bow shock. The flow conditions downstream of the bow shock are different in that the velocity, Mach number, and total pressure are decreased, the static pressure and static temperature are increased, and the total enthalpy outside the forebody boundary layer remains the same. It is this flow condition just ahead of the propulsion system, depicted in Figure 3 by M_1, that is to be duplicated by the facility free-jet exhaust. In the 8'HTT, however, it is the free-stream conditions (M_∞, $H_{t,\infty}$) which are simulated.

The flight free-stream total enthalpy is duplicated in the CHSTF heater by burning hydrogen in air with oxygen replenishment. The heated, simulated air is then expanded through the facility contoured nozzle and flows over and through the engine module at a Mach number (M_1) that simulates the vehicle forebody precompressed flow. The altitude, or dynamic pressure, simulated by the nozzle exit flow is dependent upon the heater total pressure. Also, the scramjet engine module can be mounted in the facility so that all or a portion of the facility-nozzle top-surface boundary layer is ingested by the module in partial simulation of the ingestion of a vehicle forebody boundary layer by the flight engine.

Shortcomings of Flight Simulation with Ground Facilities

Although the flight total enthalpy can be duplicated by the ground test facility, other flow properties and characteristics must be examined carefully. These facilities often have stagnation pressure limitations which result in higher altitude simulation and lower combustor pressures than desired. Also, the test gas chemistry usually does not correctly simulate the flight situation since nonequilibrium effects and contaminants are introduced into the test gas during the heating process. Contaminants include products of combustion (such as water vapor and carbon dioxide) for combustion-heated facilities and nitric oxides for arc-heated facilities. Expansion of the heated air in the facility nozzle leaves the vibrational mode in a nonequilibrium state and, above $T_{t,1}$ = 4000° R, chemical nonequilibrium (oxygen dissociation first) can occur. This nonequilibrium affects nozzle exit flow properties and parameters; i.e., P, T, ρ, M. The facility turbulence level, which is almost certainly an unknown in engine tests, could have an effect on fuel-air mixing. Engine size (scaling effect) is very important if combustion is not mixing-controlled since chemical kinetics do not scale (fuel-air mixing does scale). Facility-model interactions (usually caused by a marginal facility diffuser) can also occur which will negate data or make its interpretation difficult. Although the factors outlined above warrant caution in the interpretation of subscale scramjet ground facility data, these tests are still very important, informative, and can be performed relatively inexpensively. These tests can yield large quantities of data which are valuable in the study of combustor-inlet interaction; fuel injector size, spacing, and staging; flameholding; and thrust performance when due account is taken of the factors affecting the data.

FACILITY DESCRIPTION

An aerial photograph of the Combustion-Heated Scramjet Test Facility, showing the proximity of the test cell containing the facility, the vacuum exhaust system, and other auxiliary systems, is shown in Figure 4. Photographs of the internal portion of the test cell showing the heater, nozzle, test cabin, diffuser, etc., are shown in Figures 5 and 6. The main features of the test facility are indicated on the schematic shown in Figure 7.

The test facility is contained in a 16- by 16- by 52-foot test cell constructed of 16-in.-thick, reinforced concrete designed to contain any apparatus failure. An air intake fan is located in the test cell intake tower to provide a continuous atmospheric air purge of the test cell whenever propellant lines are pressurized and the possibility of a gaseous leak exists.

The CHSTF heater is used to increase the test gas total enthalpy for flight simulation by the combustion of hydrogen in oxygen-enriched air. The combustion occurs within an 18-inch internal diameter, 0.75-inch thick, heat-sink 201-nickel liner which is contained within a 24-inch diameter schedule-40 carbon steel pipe (Figure 8). The heat-sink nickel liner is backside cooled with air (from a 1000 psia air supply) flowing from the downstream end of the heater toward the upstream end and into the heater chamber.

The test air is supplied to the heater by a centralized 600 psig distribution system. Hydrogen and oxygen are supplied from 60,000 standard cubic feet tube trailers at

2400 psia and purge nitrogen (for pre- and post-test use) is supplied from a 47,000 scf tube trailer at 2400 psia (Figure 4). Both the hydrogen and oxygen systems can be arranged such that two trailers are connected, giving a capacity of 120,000 scf per system. Oxygen is injected across a baffle plate in the upstream end of the mixer section to ensure thorough mixing, as shown in Figure 8. Hydrogen is then injected into the oxygen-rich air mixture across a second baffle plate. Both baffle plates have 2 rings of orifices, 10 orifices in the inner ring and 20 in the outer ring, through which injector tubes pass. Ignition of the heater propellants is provided by a hydrogen-oxygen torch ignitor that is installed as shown in Figure 8. Premixing the air and oxygen results in good mixing and thus the existing length-to-diameter ratio of 3.3 is sufficient for good combustion in the heater. The design of the passages through the oxygen and hydrogen baffle plates is such that the air Mach number is about 0.9 and the air-oxygen mixture Mach number is about 0.7 through the respective baffle plates. Oxygen and hydrogen are injected through orifices at about Mach = 0.7. The facility hydrogen and oxygen flow rates are controlled so that the resulting combustion product mixture contains approximately 21 per-cent molecular oxygen by volume to simulate the oxygen content of air. The remaining test gas is a mixture of nitrogen and water vapor; higher stagnation temperatures require higher hydrogen flow rates and, thus, the water vapor content of the test gas is higher. The mass fractions of the test gas constituents for facility total temperatures corresponding to simulated flight speeds up to Mach 8 are shown in Figure 9. Mach 4 flight simulation (T_t = 1640° R) results in a nominal test gas composition of 6 percent water, 70 percent nitrogen, and 24 percent oxygen by mass; 9, 70, and 21 percent, respectively by volume, while Mach 5.5 flight simulation (T_t = 2550° R) results in a nominal test gas composition of 12 percent water, 63 percent nitrogen, and 25 percent oxygen by mass; 18, 61, and 21 percent, respectively by volume.

The test gas can be expanded from the heater through either a Mach 3.5 or a new Mach 4.7 nozzle. The Mach 3.5 nozzle (Figure 10a) is an uncooled, contoured square-cross-section nozzle designed on the basis of streamline-tracing the flow of an axisymmetric nozzle.[15,16] The throat is 4.976 in. square (throat area of 24.76 in.^{2}), and the flow exit is 13.264 in. square. The nozzle entrance, which protrudes into the heater duct, makes a transition from a circular to a square cross section. The throat section was constructed of a large mass of stainless steel for heat sink, and the downstream expansion section of the nozzle was constructed of 0.183-in.-thick carbon steel with external stiffening webs. The new Mach 4.7 nozzle (Figure 10b) is similar to the Mach 3.5 nozzle in that its contour was designed using the streamline tracing method. It has, however, a water-cooled copper throat, including the first 24 inches of the carbon steel expansion section, to allow operation at the Mach 6.0 flight stagnation temperature (3000° R). The downstream contoured section is uncooled and is fabricated by the same method as the Mach 3.5 nozzle. The throat is 2.588 inches square (throat area of 6.70 in.^{2}) and the exit has the same dimension as the Mach 3.5 nozzle, 13.264 inches square. The sidewalls and bottom wall of both nozzles are extended at the exit to ensure that shocks, generated when the ratio of test cabin to nozzle-exit static pressure becomes as high as 2.0, will not enter the internal flow region of an engine model. The nozzle extension guides the flow to provide a free-jet exhaust, 1.5 nozzle exit diameters long, to the test cabin where a subscale scramjet would be installed, as shown schematically in Figure 11. The test cabin contains the free-jet exhaust which is received by an exhaust catch cone connected to a 19-inch diameter straight duct supersonic exhaust diffuser (about 5.25 diameters long instead of the desired length of 8 diameters).[17]

The tunnel can be operated with two different exhaust modes. One mode utilizes an air-ejector to entrain and energize the tunnel flow and the other utilizes the new vacuum sphere to provide a low pressure exhaust. While operating with the air ejector, the tunnel flow (30 to 60 lbm/s) is pumped upon at the diffuser exit by the annular ejector (about 180 lbm/s) with an ejector exit Mach number of 4.16 (can be manually changed to M = 3.72). The two flows mix in a 25-inch diameter mixer duct that is about 5.5 diameters long, after which the flow is turned vertically by the turning elbow and exhausted as a free-jet to the atmosphere via a 30-inch butterfly check valve through a 6-foot diameter duct in the test cell ceiling exhaust tower (see Figure 7).

While operating with the vacuum exhaust, the air ejector is not used and the tunnel flow is exhausted to a 70-foot-diameter vacuum sphere. In this mode of operation, the 30-inch butterfly check valve (Figure 7) is automatically closed by vacuum when the fast-acting, hydraulically actuated, 48-inch vacuum valve opens and the exhaust flow is then diverted through approximately 200 feet of vacuum ducting to the sphere as shown in Figure 4. The addition of the vacuum sphere exhaust mode offers several advantages over the air ejector exhaust mode of operation. The lower pressure exhaust capability of the vacuum sphere permits higher altitude flight simulation. In addition, facility-model interactions, which occur when flow losses are high and the diffuser/air ejector system cannot adequately process the tunnel flow, should be reduced. The air ejector system also uses a large quantity of air which results in coordination problems with other facilities operating off the same central air supply. This problem is essentially eliminated with the addition of the vacuum sphere exhaust system.

Between tests, the sphere is evacuated by a three-stage steam ejector (Figure 4) which utilizes approximately 25,000 pounds of steam per hour at 300 psig supply pressure. During a nominal (tunnel flow of 30 lbm/s) 30-second run, the sphere pressure reaches about 130 mmHg (initial pressure of 10 mmHg). As shown in Figure 12, the

steam ejector can evacuate the sphere to the vacuum level required for the next test in about 20 minutes. This allows the test turn around time of 20-30 minutes achieved in the past to be maintained in which six or more tests can be conducted in a half-day test setup.

Water sprays are introduced into the tunnel flow at several strategic locations (Figure 7). First, water is sprayed into the catch cone region where the test cabin flow exhausts into the diffuser. This water spray quenches any further combustion of unburned engine fuel and helps to cool the hot exhaust for more efficient diffusion. Water is also sprayed onto the back side of the inactive air ejector nozzle lip during vacuum mode operation to cool this relatively thin metal lip. Further downstream, water is sprayed in the turning elbow to cool the turning vanes. Water is also sprayed onto the 30-inch butterfly check valve during operation with the air ejector and onto the 48-inch vacuum butterfly valve during vacuum mode operation. The water sprays also serve to cool the exhaust flow to the vacuum sphere to approximately 250° F and increase available test time. During continued tests, the necessity for all water sprays is being evaluated.

Model Installation

A subscale scramjet model (about 6 by 8 by 72 inches) is shown installed in the free-jet flow at the exit of the CHSTF nozzle in Figure 13. The scramjet model can be positioned either in the core of the free jet or flush with the facility nozzle top surface to ingest the nozzle boundary layer, thus, partially simulating the effect of vehicle forebody boundary-layer ingestion. Gaseous hydrogen fuel is supplied to the model, at pressures up to 700 psia, through six individually controlled systems. These six systems can be routed to different engine fuel injection stations for use as desired during a test. One of these systems generally controls the supply of a pyrophoric gas (20 percent silane, 80 percent hydrogen, by volume) which is used to ignite the fuel-air mixture in the engine as it is not possible to autoignite the fuel at some simulated flight conditions. Eight high-voltage electric transformers and their controls are also available as standard test options in the test cell for use with other ignitor systems which require electric sparks. Four oxygen control systems, which have been used in the past to feed hydrogen-oxygen preburners for heating hydrogen fuel prior to model injection, are available. Three additional oxygen and three hydrogen systems supplied from K-bottles are available for use with torch ignitors.

Data Acquisition System

A Modcomp 9250 32-bit computer controls data acquisition and is used to acquire and reduce test data (i.e., temperatures, pressures, forces etc.) from the facility and test model. The system provides up to 192 analog channels with input ranges of 8, 16, 32, 65 and 130 millivolts. An electronically scanned pressure (ESP) measuring system provides up to 256 pressure measuring channels with typical ranges of 15, 45 and 75 psia. Sixteen digital input channels are also available. Model thrust and drag are measured with a strain-gauge force balance or with individual load cells. A photograph of the data acquisition system and the facility control room is shown in Figure 14.

Real time parameters are displayed on two color monitors (up to 24 parameters per page on 24 pages). During tests, raw data and computed parameters can be written to tape and to disk for the purpose of more detailed analysis later. Typically, this data is stored to tape at 10 data scans per second. The maximum rate (limited by the tape drive) is 50 scans per second when only the analog channels are used, but the ESP system limits data acquisition to 20 scans per second.

Real time data, available for output after each run, are typically obtained at two data scans per second with a maximum rate of four scans per second. These data, in the form of ratios, engineering units, and/or calculations from raw data, are sent to a line printer for printed output and also to a graphics terminal and hard copy unit for quick-look plots for immediate post test analysis. These data are transferred to floppy disk for distribution and further analysis.

TEST OPERATION SEQUENCE

Air Ejector Exhaust Mode

The sequence of events during a normal scramjet test is shown in Figure 15 (Figure 15a shows the air-ejector exhaust mode and Figure 15b shows the vacuum exhaust mode). In the air ejector mode, with low tunnel flow (≈15 lbm/s) established, air ejector flow is established (≈180 lbm/s) and the tunnel air flow is brought up to the test condition (≈30 lbm/s). The heater ignitor is fired and, upon verification of good ignitor response, the timer reset circuit is energized which initiates a number of actions including hydrogen flow to the heater. Upon verification of good heater ignition (observed rise in burner temperature and pressure), the timer start circuit is energized which initiates a second string of actions including oxygen flow to the heater. Shortly after timer start, the ignitor circuit times out, thus shutting off flow to the ignitor. Typically, about 5 seconds are allowed for the facility to reach steady state operation and, following a no-fuel data acquisition period, the model fuel sequence begins. This sequence usually begins with a small flow of the silane/hydrogen gas for ignition, and is followed by a sequence of increasing hydrogen flow in timed step-function fashion to allow steady operation and data collection. Typically the model fuel is shut off 2 seconds (allows comparison of model post-burn to pre-burn conditions) before timer stop. Timer stop automatically shuts off hydrogen and oxygen flow to the heater as well as other auxiliary systems. Following timer stop the control panel is visually scanned and, upon verification that all systems are ready for shutdown (including no

indication of hydrogen by the hydrogen detectors), the air ejector flow is stopped but a small flow of tunnel air (≈15 lbm/s) continues. The facility can remain in this state until the next test or until complete facility shutdown is desired.

Vacuum Exhaust Mode

Vacuum mode operation is slightly different. After full tunnel air flow is established (≈30 lbm/s), the heater ignitor is fired. Upon verification of good ignitor operation, the timer reset circuit is energized initiating the opening of the 48-inch vacuum valve; subsequently the 30-inch check valve is sucked closed. Once the vacuum valve is fully opened, hydrogen is permitted to flow to the heater. Following observation of good heater operation, the timer start circuit is energized and oxygen flows to the heater. Again, about 5 seconds is allowed for the facility to reach steady state before the model fuel sequence is initiated. When the timer stops, all propellants are shut off and the control panel is checked to ensure that all systems are ready for shut down. Again, one of the main checks is for the presence of hydrogen via the hydrogen detectors. When all safety checks are satisfied, tunnel air flow rate is reduced to low flow (≈15 lbm/s), the vacuum valve is shut, the pressure in the tunnel builds up to the point where the 30-inch butterfly check valve automatically opens, and the tunnel continues to exhaust to the atmosphere until the next test.

TUNNEL OPERATION

After the installation of the vacuum exhaust system was completed, facility operation was checked without a model installed in the test cabin. Flow conditions throughout the facility ducting were deduced from duct wall pressure and pitot-pressure rake measurements; the relative locations of the wall and rake pressure measurements are indicated in Figure 16a. The focus of these tests was to monitor cabin pressure, and diffuser and mixer operation both in the air ejector and vacuum modes. Since the exhaust ducting configuration has changed with the addition of the vacuum leg (Figure 16a), it was necessary to confirm that the tunnel could operate in the air ejector mode in the same manner as before the modification. The vacuum mode tests verified the operational procedure of the new systems and began verification of the expanded operating envelope of the facility.

Duct Pressures

Figure 16b shows the static pressure distributions from the test cabin downstream through the diffuser and mixer section of the tunnel for the vacuum mode and the air ejector mode of operation. (The schematic of Figure 16a and the pressure distributions of Figure 16b are aligned.) The vacuum mode data corresponds to operation with a sphere inlet pressure of 1.6 psia (sphere inlet pressure was measured in the 48-inch vacuum ducting just upstream of the sphere) corresponding to a sphere pressure of approximately 0.85 psia since the duct exit to the sphere is choked at low sphere pressure. The pressure distribution through the diffuser section is similar for both modes of operation, but the pressures in the mixer section are much lower in the vacuum mode. In the air ejector exhaust mode the mixer exit pressure is atmospheric, while in the vacuum exhaust mode the pressure is below 5 psia. In addition, the mass flow through the mixer section is only the tunnel flow (30 lbm/s) while the air ejector adds an additional 180 to 200 lbm/s in the air ejector exhaust mode. When additional flow losses occur as heat is added during fueled engine tests, the low mixer mass flow and pressures in the vacuum mode will provide a larger margin before the diffuser and cabin pressure begin to rise, thus reducing the occurrence of facility-model interaction. This will be even more important with the planned addition of a Mach 6 facility nozzle, which will require a lower cabin pressure.

In the air ejector exhaust mode, the pressure distribution through the diffuser and upstream section of the mixer show normal operation when compared with data obtained before the facility modification, but a pressure oscillation occurs in the downstream section of the mixer just ahead of the turning elbow. The nature of this oscillation is indicated by the pitot pressure profile (Figure 17—indicated cycle numbers are at 0.5-second increments) measured just upstream of the turning elbow (see Figure 16a for location of pitot rake). The flow profile is oscillatory where the flow is first attached along the top of the duct (and separated on the bottom) and 1-1/2 seconds later is separated along the top of the duct (and attached on the bottom). This flow phenomena perhaps can be explained as "the organ pipe effect" where the dead-end section of pipe leading to the vacuum sphere develops a pressure oscillation. The typical flow profile prior to the addition of the vacuum ducting was with separated flow at the top of the duct as the tunnel flow passed through the outside area of the elbow exhausting to the atmosphere. However, in the new configuration the flow going past the dead-end Y-section of pipe (Figures 7 and 16a) entrains the air in the vacuum leg, reducing the pressure in the dead-end Y-section to the point that the flow becomes attached to the inside flow area of the elbow and becomes attached to the top side of the duct and detached on the duct bottom. This flow path causes the pressure to rise in the dead-end leg, thus starting the cycle over, that is, allows the flow to return to its normal flow path to the elbow outer flow region. This pressure cycle is theorized to be causing the oscillation of the flow profile in the downstream mixer section. More instrumentation is being added to the tunnel in an attempt to confirm this theory. If confirmed, the problem can probably be remedied by adding a protrusion in the downstream mixer section of the ducting to stabilize the flow.

The flow conditions discussed above resulted from tests conducted without a model installed in the tunnel. In general, the installation of a model causes any marginal operation to worsen due to the increased total pressure losses and flow asymmetry. Data with a model installed will be

necessary to fully confirm tunnel operation. Data obtained to date, however, suggest that tunnel operation with the vacuum mode exhaust should be improved relative to previous operation with the air ejector in terms of reduced facility-model interaction and lower cabin pressure (thus, higher altitude simulation capability).

Test Time

Several factors limit test duration in this type of facility. Most of these factors result from the use of heat-sink, instead of actively-cooled, components such as the heater liner, nozzle throat, and the test model. Both the air ejector and vacuum mode of operation introduce specific limitations. In the air ejector mode, where air usage is high, a limit on run time exists due to bottle field air supply pressure and coordination with other facilities that utilize the same air supply. In the vacuum mode, a limit exists due to sphere capacity. As the sphere pressure rises during a run, the diffuser flow will start to break down at some point in time, the cabin pressure will be affected, and the test condition will no longer be steady.

An attempt was made to quantify this limiting sphere pressure and examine the process of diffuser breakdown during unheated flow tests where tunnel flow rate was typical (≈30 lbm/s) of that for heated flow tests, but the heater was not operated and the tunnel total pressure was about 50 psia instead of about 92 psia. Shown in Figure 18 are traces of the cabin, diffuser, and mixer pressures as the sphere inlet pressure rises. This data is a time composite of four separate test runs. The mixer pressure starts to rise after about 50 seconds of test time or at a sphere inlet pressure of about 1.8 psia. The diffuser exit pressure starts to rise at a sphere inlet pressure of about 3.8 psia and the diffuser entrance pressure begins to rise at a sphere inlet pressure of about 5.2 psia. Once the diffuser entrance pressure begins to rise the cabin pressure almost immediately follows, signaling the end of steady-state test conditions. It is important to realize two things about these data: no model was installed during the test and the test was conducted with unheated flow. Thus, total pressure losses were at a minimum (due to the absence of a test model), but the initial total pressure of the flow was much lower than with a normal test in which the heater is operated (≈50 psia instead of ≈92 psia). In addition, when the exhaust flow is hot, the sphere pressure will rise more rapidly than indicated by this unheated flow test, but the characteristics of the flow relative to the sphere inlet pressure are believed to be representative.

NOZZLE CALIBRATION

Nozzle exit pitot pressure and total temperature surveys were performed on the Mach 3.5 nozzle. Wall static pressures were also measured and used in conjunction with the nozzle exit surveys to calculate the remaining flow-field parameters. Horizontal Mach number profiles determined from the nozzle exit measurements are shown at several locations across the nozzle exit flow field in Figure 19. The vertical centerline profile is plotted in Figure 20 along with a profile from a CFD solution of the nozzle flow field, performed using the Spark 3-D Navier Stokes code developed at NASA LaRC.[18] The CFD solution was performed on one quarter of the flow field, and symmetry was assumed for the remainder of the square-cross-section nozzle exit flow field. Good agreement can be seen between the CFD solution and the data. Mach number nozzle exit contours generated from the CFD solution are shown in Figure 21 along with an outline of a typically installed engine. The contour shows a fairly uniform core flow with the effects of vortical corner flow. This exit contour is typical of the flow field produced by these square cross sectioned nozzles.[19,20] Experimental and CFD integrated mass flow computations agreed within 3 percent at a nominal flow rate of 30 lbm/s.

OPERATIONAL ENVELOPE

Expanded Simulation of CHSTF

The expanded flight simulation capabilities of the Combustion-Heated Scramjet Test Facility are shown in Figure 22. The parameters limiting the simulation envelope are indicated. Increasing the heater pressure capability from 190 psia to 500 psia increased the flight dynamic pressure which could be achieved at a given Mach number. This limit is outlined by the 500 psia heater pressure line. The combination of the new Mach 4.7 nozzle and the increased temperature limit of the heater to 3000° R, increased the flight Mach number simulation capability from Mach 4 to Mach 6. The temperature limit essentially limits flight Mach number simulation, as shown in the figure, and the availability of different Mach number nozzles limits the Mach number simulation entering the engine module. The addition of the vacuum sphere increased the altitude simulation capability from the air ejector limit shown in the figure to the 250 psf flight dynamic pressure boundary. This limit has not been fully defined since no engine tests have been completed to this point.

Relationship to Langley Scramjet Complex

With the CHSTF modifications discussed in this paper and the completion of the modifications to the 8'HTT, the simulation envelopes of the facilities in the Langley Scramjet Test Complex now overlap as shown earlier in Figure 2. With the NASP program moving towards the flight of an experimental aircraft, the X-30, the need for projected flight performance of scramjet engines is becoming critical. To date, the real focus of the subscale engine tests performed in the ground facilities has been towards component integration. The projection of these results to obtain the performance of a full scale engine in flight conditions is a very difficult task. Many of the problems discussed before, including test gas contamination and nonequilibrium, kinetics problems, scaling problems, etc.,

are difficult to analyze without a basis for comparison. With the overlap in facility simulation capabilities, two tests run at similar conditions in different facilities can be compared. For example, tests in the CHSTF and AHSTF at similar conditions can be used to compare the effects of different test gas contamination (H_2O for the CHSTF and NOx for the AHSTF) on performance. Since the 8'HTT conditions overlap the test conditions both the CHSTF and AHSTF, scaling effects can be studied. With such effects as scaling and test gas contamination better understood, the difficult task of projecting ground test data to a flight condition will be made easier.

SUMMARY

The modifications to the Combustion-Heated Scramjet Test Facility (CHSTF) are complete, shakedown tests are being completed, and the facility is ready to retain its operational status. The modifications included a new heat-sink nickle liner heater, a new Mach 4.7 nozzle, and a new 70-foot vacuum sphere exhaust system. A description of the facility was presented along with a discussion of data results from the shakedown tests.

Data results indicate that the facility in the air ejector mode of operation performed similarly to that prior to the addition of the vacuum sphere ducting. Vacuum sphere mode of operation resulted in much lower mixer duct pressures that will be beneficial in minimizing facility/model interactions and allow higher Mach number nozzles to be utilized. Mach 3.5 nozzle exit survey data were presented and flow profiles were shown to compare favorable with CFD-generated flow profiles.

The overall expanded envelope of the flight simulation capability of the CHSTF was described. The CHSTF, the Arc-Heated Scramjet Test Facility, and the 8-Foot High-Temperature Tunnel (8'HTT) comprise the NASA Langley Scramjet Test Complex. After the completion of these CHSTF modifications and the modifications being made to the 8'HTT, the simulated envelopes of these three facilities will overlap. The relationship between the simulated envelopes of all three facilities was shown and the importance of their overlap was discussed.

REFERENCES

[1]Hypersonic Research Engine Project - Phase II Structures and Cooling Development Final Technical Data Report. NASA CR-112087, May 1972.

[2]Hypersonic Research Engine Project - Phase II Aerothermodynamic Integration Model Development Final Technical Data Report. NASA CR-132654, May 1975.

[3]Hypersonic Research Engine Project - Phase II Aerothermodynamic Integration Model (AIM) Test Report. NASA CR-132655, May 1975.

[4]Henry, John R.; and Anderson, Griffin Y.: Design Considerations for the Airframe-Integrated Scramjet. NASA TM X-2895, December 1973.

[5]Andrews, Earl H., Jr.; Torrence, Marvin G.; Anderson, Griffin Y.; Northam, G. Burton; and Mackley, Ernest A.: Langley Mach 4 Scramjet Test Facility. NASA TM-86277, 1985.

[6]Guy, Robert W.; Torrence, Marvin G.; Sabol, Alexander P.; and Mueller, James N.: Operating Characteristics of the Langley Mach 7 Scramjet Test Facility. NASA TM-81929, 1981.

[7]Thomas, Scott R.; and Guy, Robert W.: Expanded Operational Capabilities of the Langley Mach 7 Scramjet Test Facility. NASA TP-2186, 1983.

[8]Guy, Robert W.; Pinckney, S. Zane; and Andrews, Earl H., Jr.: Summary of NASA Langley's Scramjet Engine Tests. 1985 JANNAF Propulsion Meeting, Publication No. 425, April 9-12, 1985. (Conf.)

[9]Andrews, Earl H., Jr.: A Subsonic to Mach 5.5 Subscale Engine Test Facility. AIAA Paper 87-2052, June 1987.

[10]Kelly, N. H.; and Wieting, A. R.: Modification of NASA Langley 8-Foot High Temperature Tunnel to Provide a Unique National Research Facility for Hypersonic Air-Breathing Propulsion Systems. NASA TM-85783, May 1984.

[11]Reubush, D. E.; and Puster, R. L.: Modification to the Langley 8-Foot High-Temperature Tunnel for Hypersonic Propulsion Testing. AIAA Paper 87-1887, July 1987.

[12]Andrews, Earl H.: Scramjet Test Complex. Langley Aerospace Test Highlights, NASA TM-87703, p. 34, 1985.

[13]Northam, G. Burton; and Anderson, G. Y.: Supersonic Combustion Ramjet Research at Langley. AIAA Paper 86-0159, January 1986.

[14]Russin, William Roger: Performance of a Hydrogen Burner to Simulate Air Entering Scramjet Combustors. NASA TN D-7576, 1974.

[15]Evvard, John C.; and Maslen, Stephen H.: Three-Dimensional Supersonic Nozzles and Inlets of Arbitrary Exit Cross Section. NACA TN 2688, 1952.

[16]Beckwith, Ivan E.; and Moore, John A.: An Accurate and Rapid Method for the Design of Supersonic Nozzles. NACA TN 3322, 1955.

[17]Andrews, E. H., Jr.; and Mackley, E. A.: Design, Tests and Verification of a Diffuser System for a Mach 4 Scramjet Test Facility. J. Aircraft, vol. 16, no. 10, October 1979, pp. 641-642. (Available as AIAA Paper 78-771, revised.)

[18]Drummond, J. P.; and Hussaini, M. Y.: Numerical Simulation of a Supersonic Reacting Mixing Layer. AIAA Paper 87-1325, June 1987.

[19]Thomas, Scott R.; Voland, Randall T.; and Guy, Robert W.: Test Flow Calibration Study of the Langley Arc-Heated Scramjet Test Facility. AIAA Paper 87-2165, June 1987.

[20]Ostrander, Mark J.; Thomas, Scott R.; Voland, Randall T.; Guy, Robert W.; and Srinivasan, Shivakumar: CFD Simulation of Square Cross-Section, Contoured Nozzle Flows: Comparison With Data. AIAA Paper 89-0045, January 1989.

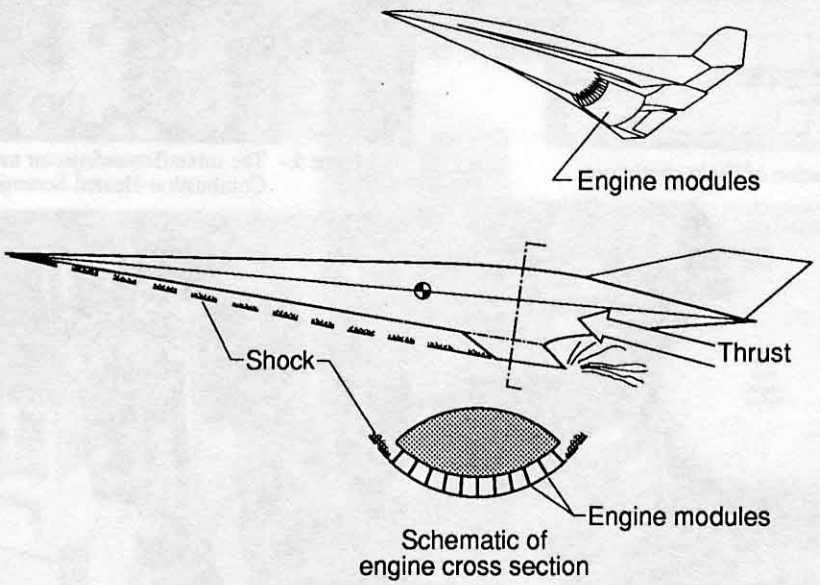

Figure 1.- Airframe-propulsion system integration.

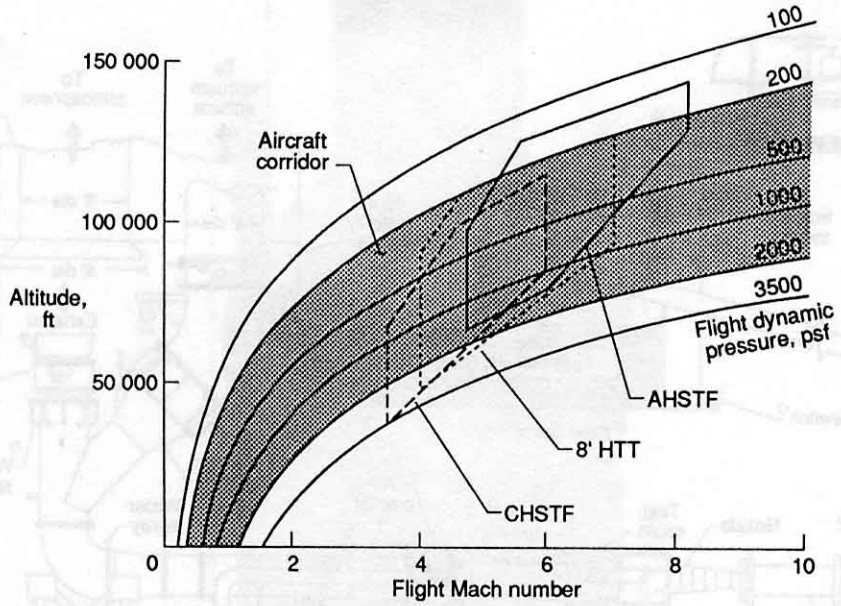

Figure 2.- Test capability of NASA Langley scramjet test facilities.

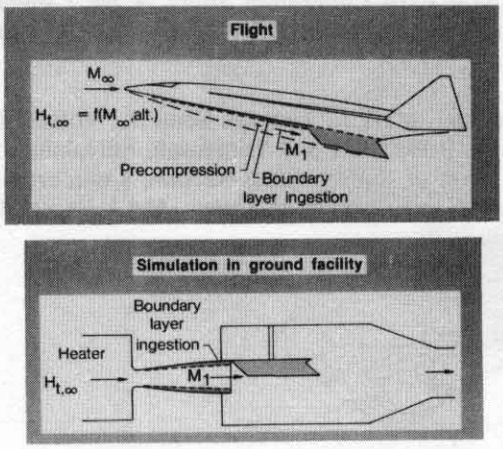

Figure 3.- Simulation of flight conditions.

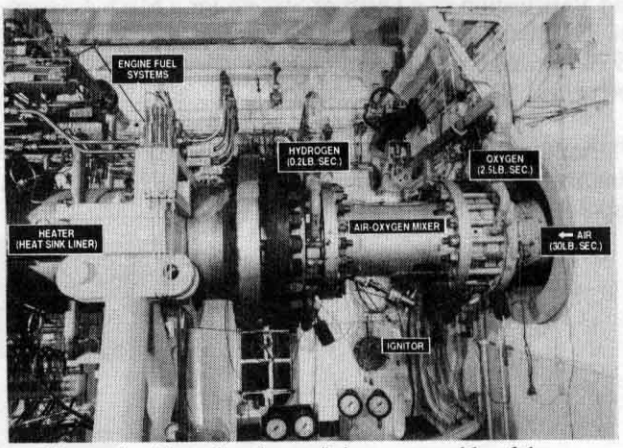

Figure 5.- The mixer/heater/injector assembly of the Combustion-Heated Scramjet Test Facility.

Figure 4.- The NASA Langley hypersonic propulsion scramjet test cell complex.

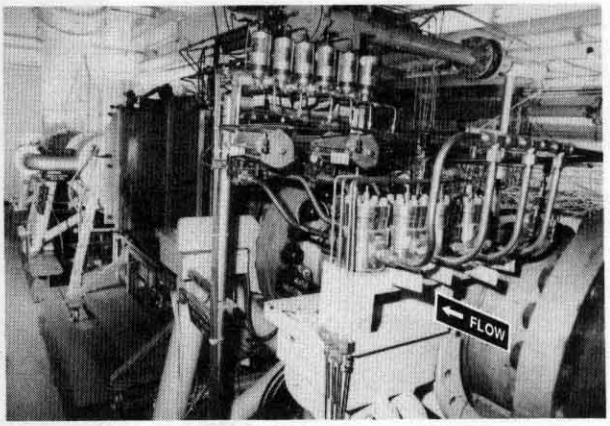

Figure 6.- An overall view in the test cell of the Combustion-Heated Scramjet Test Facility.

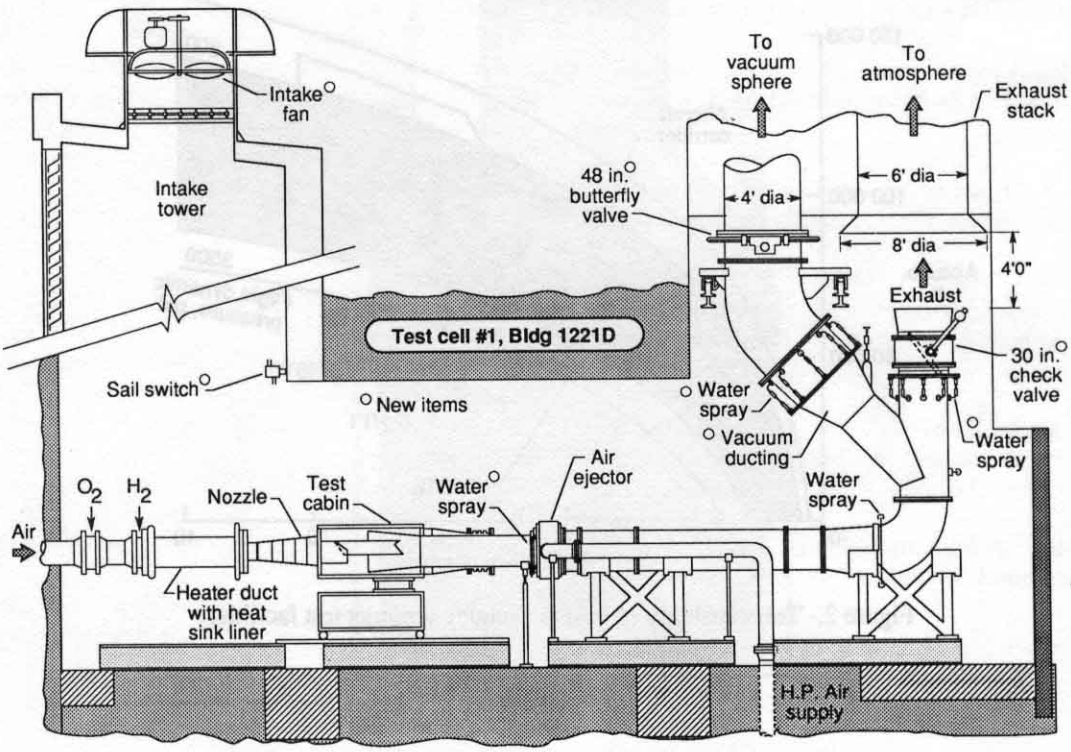

Figure 7.- Schematic of the Combustion-Heated Scramjet Test Facility.

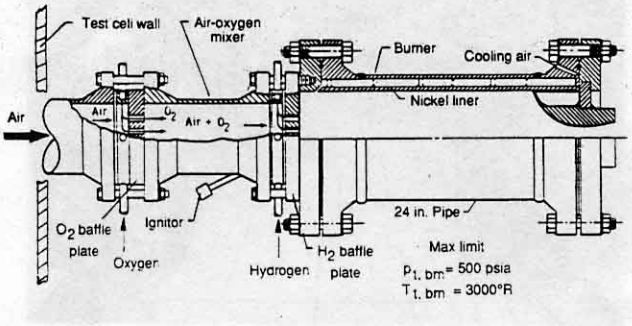

Figure 8.- Schematic of the mixer/heater/injector assembly

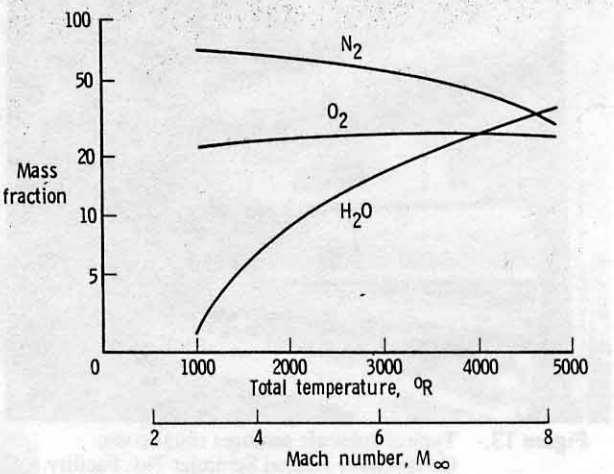

Figure 9.- Test gas constituents; hydrogen-air combustion with oxygen replinishment.

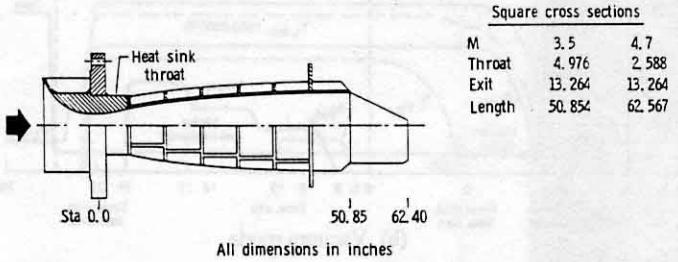

Square cross sections

M	3.5	4.7
Throat	4.976	2.588
Exit	13.264	13.264
Length	50.854	62.567

(a) Mach 3.5

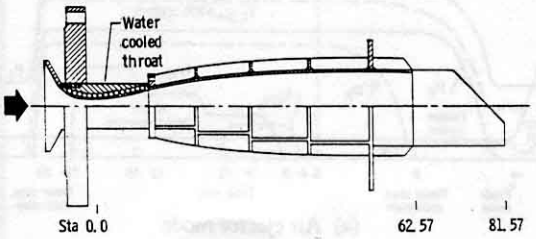

(b) Mach 4.7

Figure 10.- Facility supersonic nozzles.

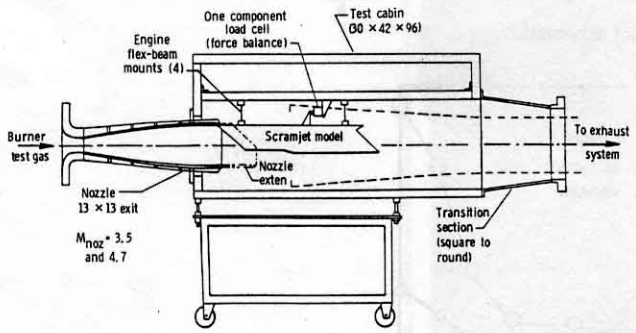

Figure 11.- Schematic of a subscale scramjet test setup; standard configuration.

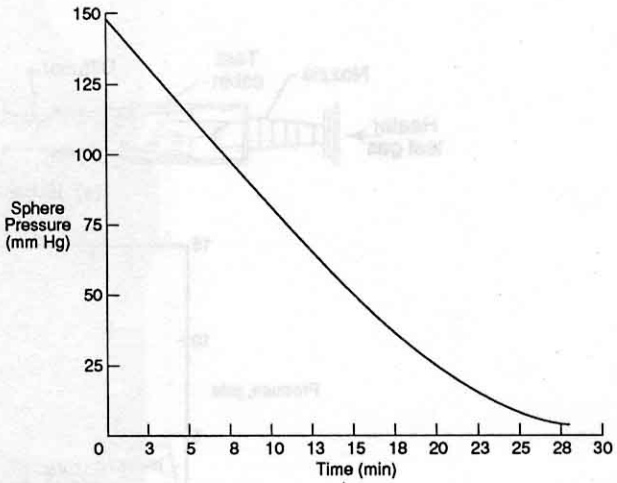

Figure 12.- Stream ejector/sphere pump down rate.

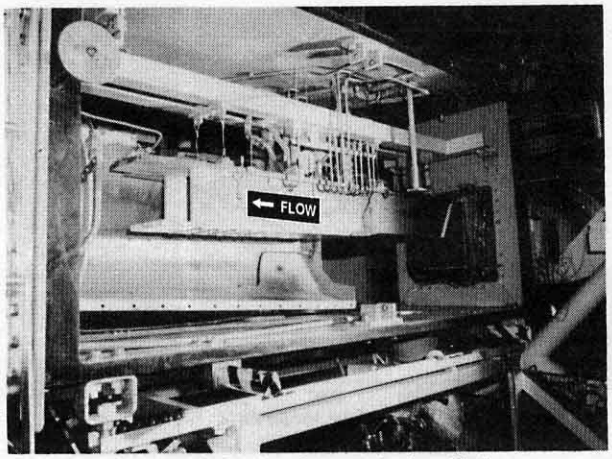

Figure 13.- Typical subscale scramjet installation; Combustion-Heated Scramjet Test Facility.

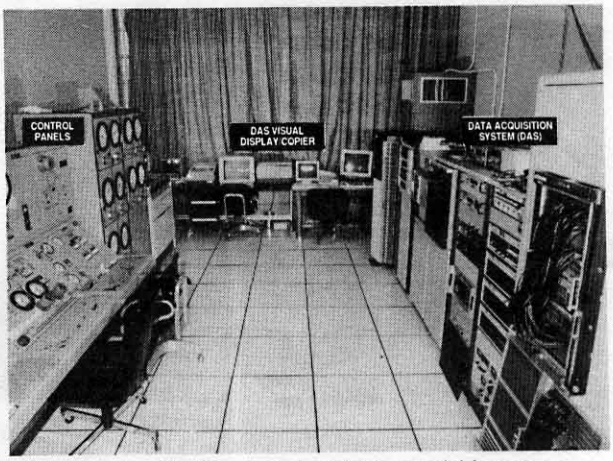

Figure 14.- Facility control and data acquisition room; Combustion-Heated Scramjet Test Facility.

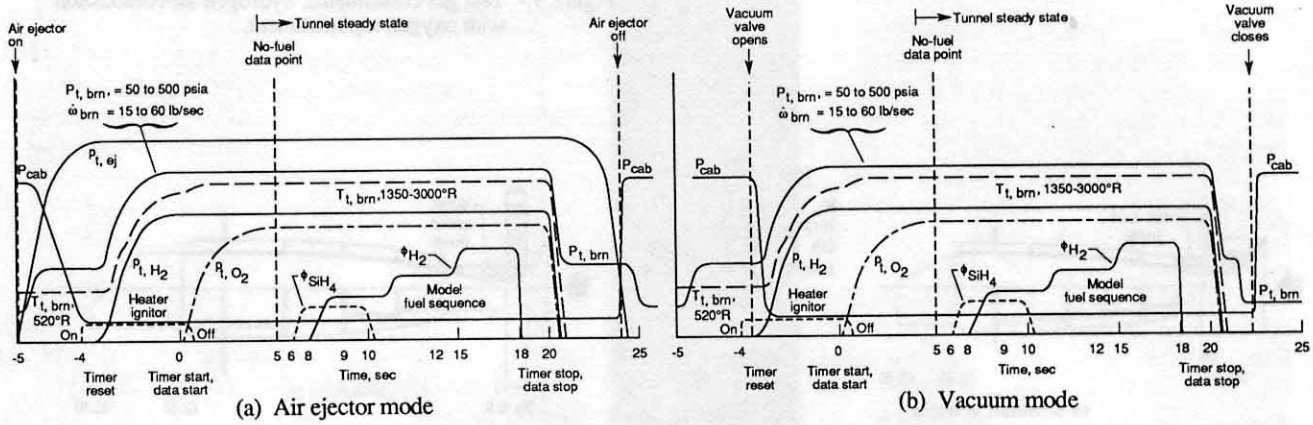

(a) Air ejector mode

(b) Vacuum mode

Figure 15.- Typical run sequence; Combustion-Heated Scramjet Test Facility.

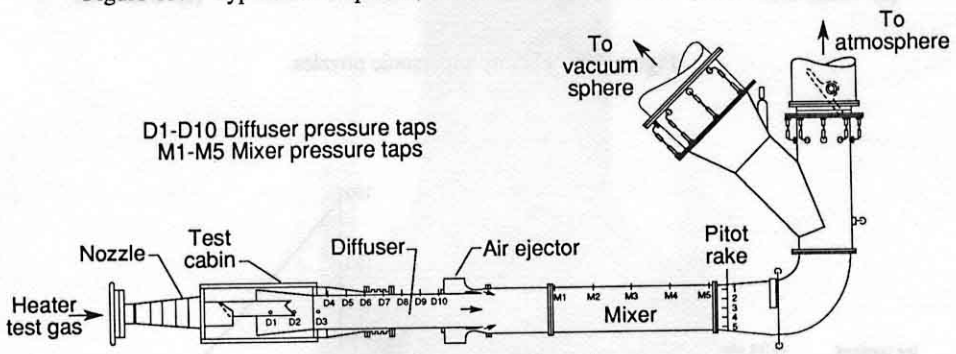

(a) Exhaust duct schematic

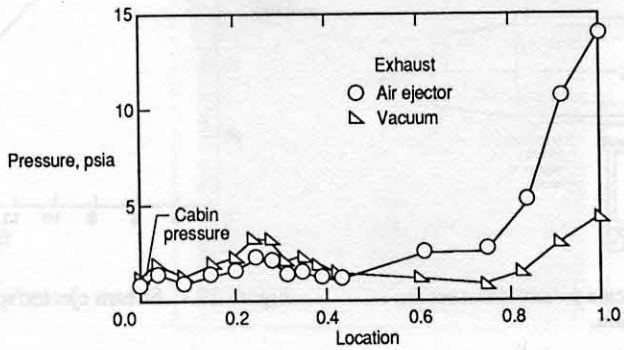

(b) Pressure distributions

Figure 16.- Facility exhaust duct schematic and pressure distributions.

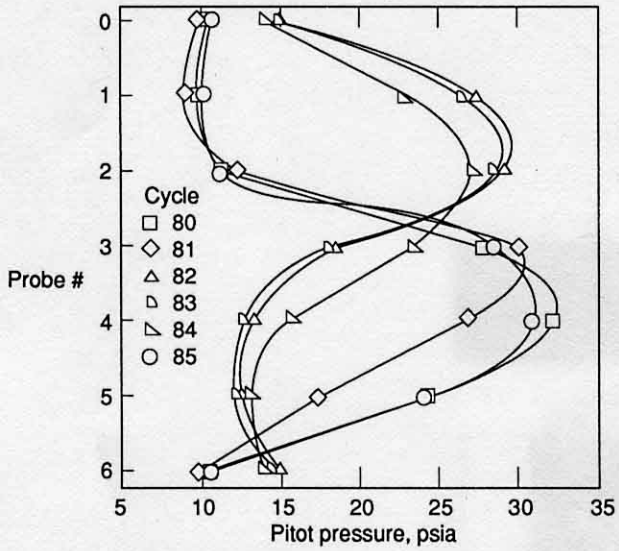

Figure 17.- Exhaust duct mixer exit flow pitot pressure profile.

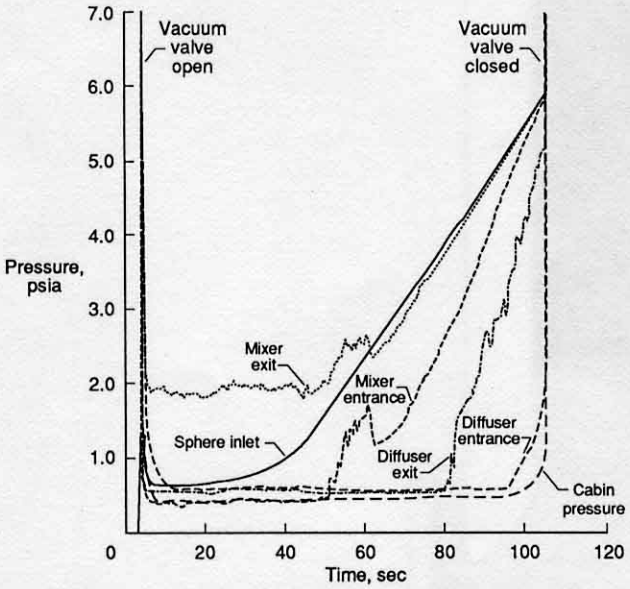

Figure 18.- Facility static pressure time history plots.

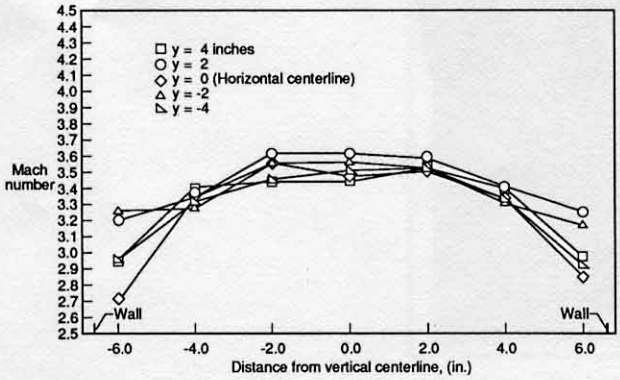

Figure 19.- Mach 3.5 nozzle exit Mach number horizontal profiles; experimental data.

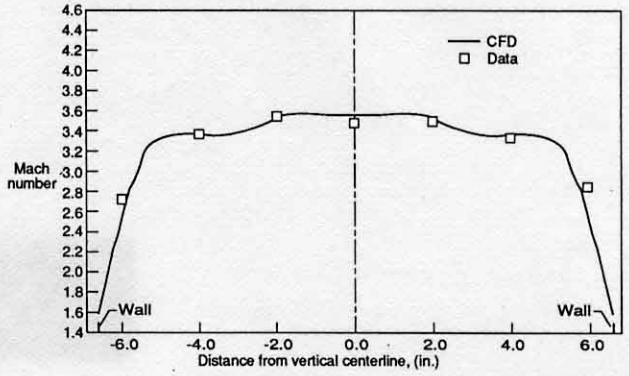

Figure 20.- Mach 3.5 nozzle exit Mach number profiles; CFD/data comparison, horizontal centerline.

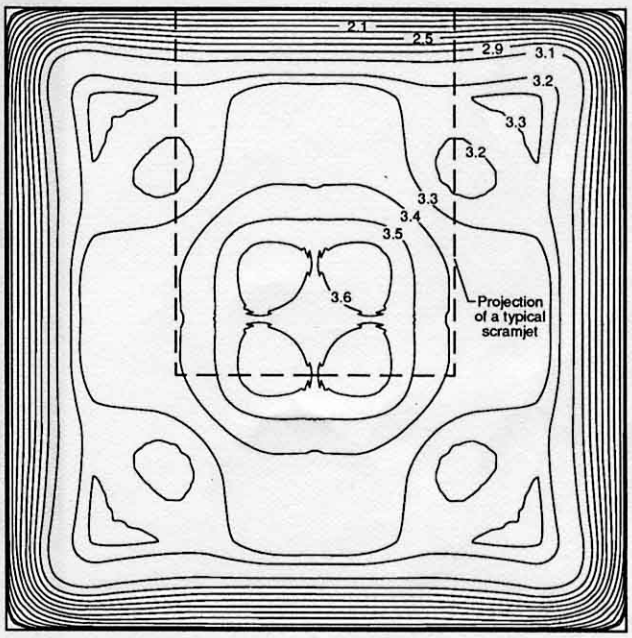

Figure 21.- Mach 3.5 nozzle exit Mach number contours.

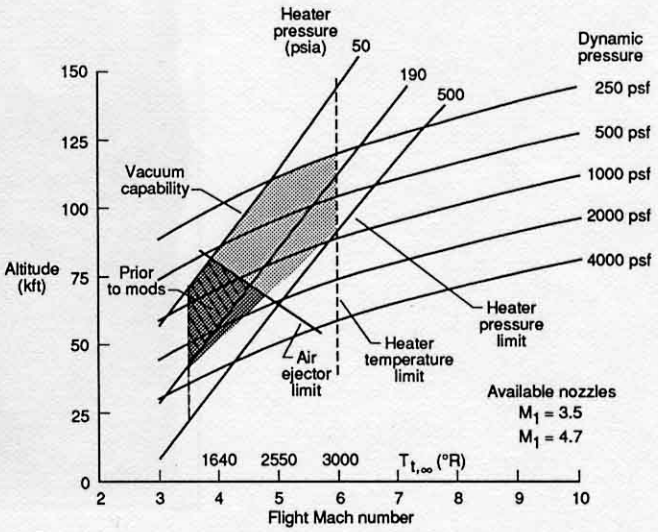

Figure 22.- Expanded operational envelope; Combustion-Heated Scramjet Test Facility.